Energy Efficient and Adaptive Design for Wireless Power Transfer in Electric Vehicles

Xiaolin Mou, Oliver Groling, Andrew Gallant and Hongjian Sun
School of Engineering and Computing Sciences, Durham University, Durham, UK
Email: hongjian.sun@durham.ac.uk

***Abstract*—Wireless power transfer (WPT) could revolutionize global transportation and accelerate growth in the Electric Vehicle (EV) market, offering an attractive alternative to cabled charging. Coil misalignment is inevitable due to driver parking behaviour and has a detrimental effect on power transfer efficiency (PTE). This paper proposes a novel coil design and adaptive hardware to improve PTE in magnetic resonant coupling WPT and mitigate coil misalignment, a crucial roadblock in its acceptance. The new design was verified using ADS, providing a good match to theoretical analysis. Custom designed receiver and transmitter circuitry was used to simulate vehicle and parking bay conditions and obtain PTE data in a small-scale setup. Experimental results showed that PTE can be improved by 30% at the array's centre, and an impressive 90% when misaligned by 3/4 of the arrays radius. The proposed novel coil array achieves overall higher PTE compared to the benchmark single coil design.**

***Index Terms*—wireless power transfer, magnetic resonant coupling, electric vehicle, power transfer efficiency, misalignment, coil design, adaptive hardware**

I. Introduction

Wireless power transfer (WPT) technologies can be dated back to the early 20th century, i.e. Nikola Tesla, a pioneering electronic engineer who invented the Tesla Coil. Much research in recent years has focused on WPT technologies. In 2007, the WiTricity project at MIT demonstrated 60 W power transmission across a 2 metre air gap to light up a light bulb. They used two coils with 60 cm diameter and achieved 90% PTE [1]. Nowadays, WPT technologies are attracting widespread interest in fields such as home electronics, medical implants, EV's and the aerospace industry.

WPT technologies can be categorised into three groups, namely inductive coupling, magnetic resonant coupling (MRC), and electromagnetic radiation-based WPT [2]. MRC-WPT is advantageous with respect to its high safety and longer transmission distance [3]. Thus it plays an important role in the design of wireless EV charging systems. There are two interesting fields in WPT for EV applications: static and dynamic charging WPT. For the static scenario, the EV may be charged in a modified car park or garage. In a dynamic WPT system the EV is continuously charged in a dedicated charging lane using multiple coils embedded in the road. This makes charging more convenient and could result in downsized batteries, reducing their required capacity by 20% and permitting shorter charging times [4].

In general, WPT requires accurate alignment between the transmitter and receiver coils. The latter one is mounted on the EV to power and operate various devices.

This poses two main technical challenges:

- Standardization of transmitter (TX) & receiver (RX) coil dimensions to ensure compatibility with a wide range of EV models.
- Compensating for driver behaviour, since misalignment between TX and RX coils is inevitable in both static and dynamic charging.

The misalignment issue is critical since the electromagnetic energy in conventional MRC-WPT rapidly decays with distance between coils. Lateral and angular misalignment analysis for inductive coupling WPT has been examined by Kyriaki [5]. Previous research has been conducted to address the effect of coil design in misalignment scenarios [6] [7] [8], however, no methodology was given to mitigate the issue and no recommendations were made for an economical design to solve the problem once and for all.

To address these challenges this paper proposes a new coil design and adaptive hardware. The key contributions are:

- A new method for calculating the PTE in a laterally misaligned coil arrangement
- A novel TX coil array design for mitigating coil misalignment that improves the PTE in wireless charging EV systems
- Hardware prototype for evaluating and verifying the new coil array design

Section II introduces the underlying theory behind MRC-WPT and the mathematical model for misalignment. Section III introduces the TX coil array design and a small scale hardware prototype containing adaptive circuitry. Section IV discusses simulation results of the model and compares these to experimental data obtained by testing the hardware.

II. Theory

A. Perfect Alignment Case

A typical MRC-WPT system consists of four components: a source coil, a primary resonant coil (TX), a secondary resonant coil (RX) and a load coil, as shown in Fig. 1. The subscripts S, P, Q and W denote the source coil, the primary resonant coil, the secondary resonant coil and the load coil respectively.

D is the distance between the two resonant coils P and Q. The parameter r is the coil loop radius and the parameter a is the wire radius of the resonant coils. Resonant-based WPT enables efficient power transfer over acceptable distances by tuning the capacitive and inductive parameters of both RX and TX circuits to a common natural resonant frequency.

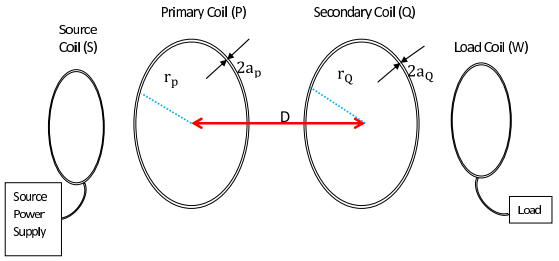

Fig. 1: Block Diagram of Magnetic Resonant Coupling WPT: source coil, primary resonant coil (TX), secondary resonant coil (RX), and load coil [9]

Assuming that the loop radii of the two resonant coils are identical, i.e. a_P=a_Q, the self-inductance L, the ohmic resistance R_o, the radiation resistance R_r and the capacitance C can be expressed as [9]:

$$L = r\mu_0\mu_r\left[ln\frac{8r}{a} - 1.75\right] \tag{1}$$

$$R_o = \sqrt{\frac{\omega\mu_0\mu_r}{2\sigma}}\frac{r}{a} \tag{2}$$

$$R_r = 20\left\{\left[\frac{2f\pi}{c}\right]^2 \cdot r^2\pi\right\}^2 \tag{3}$$

$$C = \frac{1}{(2f\pi)^2 L} \tag{4}$$

where, μ_0 is the permeability of free space, ω = 2πf, μ_r is the relative permeability, c is the speed of light, σ is the conductivity of the conductor and f is the resonant frequency. The total resistance of the resonant coil is $R = R_0 + R_r$. Equation (4) indicates that the capacitance C is determined by the self-inductance L of the resonant coil and the resonant frequency f. The PTE η can be defined as [9]:

$$\eta = \frac{\frac{\Gamma_W}{\Gamma_Q}\frac{K^2}{\Gamma_P\Gamma_Q}}{(1+\frac{\Gamma_W}{\Gamma_Q})^2 + (1+\frac{\Gamma_W}{\Gamma_Q})\frac{K^2}{\Gamma_P\Gamma_Q}} \tag{5}$$

$$\Gamma = \frac{R}{2L}, K = \frac{M\omega}{2\sqrt{L_P L_Q}} \tag{6}$$

where Γ is the intrinsic decay rate, K is the coupling coefficient between the two resonant coils and M is the mutual inductance. When the centre of the RX resonant coil is aligned with the centre of the TX resonant coil, the mutual inductance M can be given by:

$$M = \frac{\mu_0\pi(r_P r_Q)^2}{2(D^2 + r_P^2)^{\frac{3}{2}}} \tag{7}$$

The PTE η is maximized when $\Gamma_W = \Gamma_Q\sqrt{1+(K^2/\Gamma_P\Gamma_Q)}$, and can be rewritten as[9]:

$$\eta = \frac{\sqrt{1+(\frac{K}{\Gamma})^2} - 1}{\sqrt{1+(\frac{K}{\Gamma})^2} + 1} \tag{8}$$

In practice, the size of the TX and RX resonant coils may be different or they are in a misaligned position.

B. Misalignment Case

In MRC-WPT systems, the power of the TX resonant coil is transmitted to the RX resonant coil through an alternating magnetic field. Numerous experiments have established that the location of two resonant coils can affect the PTE of the whole system.

As proposed by Kyriaki [5], there are two types of misalignment referred to as lateral and angular misalignment. Lateral misalignment involves both horizontal Δ and vertical displacement D in a parallel plane between the centres of the primary and secondary resonant coils, as shown in Fig. 2. In angular misalignment the plane of the RX resonant coil is tilted at an angle ϑ and the coils are coaxial. Since angular misalignment is less likely to occur in a practical EV scenario, this paper only considers the lateral case.

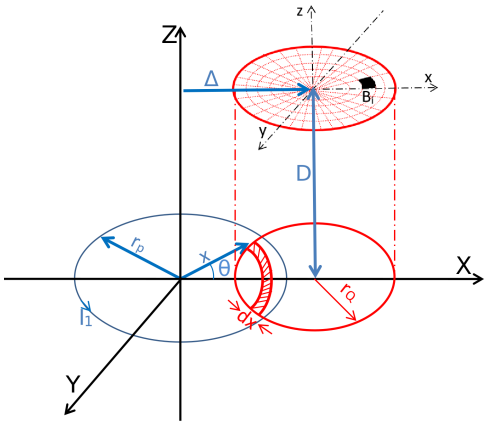

Fig. 2: Illustration of lateral misalignment between coils where r_p is the radius of TX coil, r_Q is the radius of RX coil and Δ is the lateral misalignment distance. x is the distance between the origin and magnetic field intensity area of the receiver, which has a width of d_x and subdivision magnetic field intensity of B_i.

As shown in Fig. 2, the RX resonant coil is subdivided into several identical subdivisions and r_Q is its radius. The mutual inductance between the TX and RX resonant coil M_{12} can be defined as:

$$M_{12} = \frac{N_1 N_2}{\mathbf{I_1}}\int_{\Delta-r_Q}^{\Delta+r_Q} B_i(z)\cdot 2x\arccos\frac{x^2+\Delta^2-r_Q^2}{2x\Delta}d_x \tag{9}$$

where N_1 and N_2 are the number of turns of the TX and RX resonant coils respectively. In the case of a single loop, N_1=N_2=1. $\mathbf{I_1}$ is the current in the TX resonant coil and x is the distance between the origin of the TX coil and the magnetic field intensity area on the RX coil. This area can be considered as an arc with a width of d_x. $B_i(z)$ is the subdivision magnetic field intensity and is given by equation 11. If the TX and RX resonant coils are perfectly aligned, the magnetic field intensity B is given by $\frac{\mathbf{I_1}\mu_0\mathbf{r_P^2}}{2(r_P^2+D^2)^{\frac{3}{2}}}$ and M_{12} equals $\frac{\mu_0 r_P^2}{2(r_P^2+D^2)^{\frac{3}{2}}} \cdot r_Q^2\pi$.

In the case of misalignment, B_i can be expressed in terms of cylindrical coordinates (ρ,φ,z), where r_P is the radius of the TX resonant coil and ρ and z are the displacements in the horizontal and vertical directions respectively. According to Biot-Savart's law, B_i can be written as:

$$B_i(\rho) = \frac{\mu_0 I z}{2\rho\pi} \cdot \frac{1}{\sqrt{(r_P+\rho)^2+z^2}} \cdot \left[-F(k) + \frac{r_P^2+\rho^2+z^2}{(r_P-\rho)^2+z^2} \cdot E(k)\right] \tag{10}$$

$$B_i(z) = \frac{\mu_0 I}{2\pi} \cdot \frac{1}{\sqrt{(r_P+\rho)^2+z^2}} \cdot \left[F(k) + \frac{r_P^2-\rho^2-z^2}{(r_P-\rho)^2+z^2} \cdot E(k)\right] \tag{11}$$

where, ρ and z are displacement in horizontal direction and vertical direction respectively. φ-directed fields are zero. $F(k)$ and $E(k)$ are the complete elliptical integrals of the first and second kinds respectively, where k is the modulus. Both equations of the complete elliptical integrals can be given below:

$$F(k) = \int_0^{\pi/2} \frac{d_\alpha}{\sqrt{1-k^2 sin^2(\alpha)}} \tag{12}$$

$$E(k) = \int_0^{\pi/2} \sqrt{1-k^2 sin^2(\alpha)} d_\alpha \tag{13}$$

$$k = \sqrt{\frac{4 r_P \rho}{(r_P+\rho)^2+z^2}} \tag{14}$$

The mutual inductance M_{12} can be rewritten as:

$$M_{12} = \frac{N_1 N_2}{\mathbf{I_1}} \int_{\Delta-r_Q}^{\Delta+r_Q} B_i(z) \cdot 2x \sqrt{\frac{r_Q^2-(x-\Delta)^2}{\Delta \cdot x}} d_x \tag{15}$$

M_{12} is a crucial parameter in calculating the PTE of a misaligned MRC-WPT system. The equation for PTE can be obtained by substituting (15) into (6) and subsequently into (8), however it was omitted from this paper due to its complexity and length.

III. Novel Coil Design & Hardware Implementation

In order to improve the PTE of MRC-WPT in EV's, a new primary resonant coil array was designed, which can achieve a higher PTE compared to the traditional single coil benchmark. More importantly, it can solve the misalignment issue.

Additional hardware was designed as shown in Fig. 3 to obtain experimental data and verify simulation results as discussed in Section IV. It consists of the following parts:

- 3D printed array with seven 22 mm radius TX coils
- 65 mm radius TX PCB coil for benchmark comparison
- TX & RX PCB's to simulate charger and EV respectively
- 7-channel relay PCB for selecting optimum TX coil

The vehicle-mounted power receiver measures received power P_{rx} at the load using precision RMS-DC converters, whilst the parking bay transmitter monitors transmitted power P_{tx}. XBee RF modules based on the ZigBee IEEE 802.15.4 protocol are used to establish a wireless feedback loop between the EV and parking bay. An ATMega328 microcontroller (MCU) on the TX side then calculates the current PTE. Embedded software written in C iteratively switches power to each of the coils using mechanical relays, until it finds the optimum alignment between TX and RX coils giving maximum coupling - an algorithmic approach.

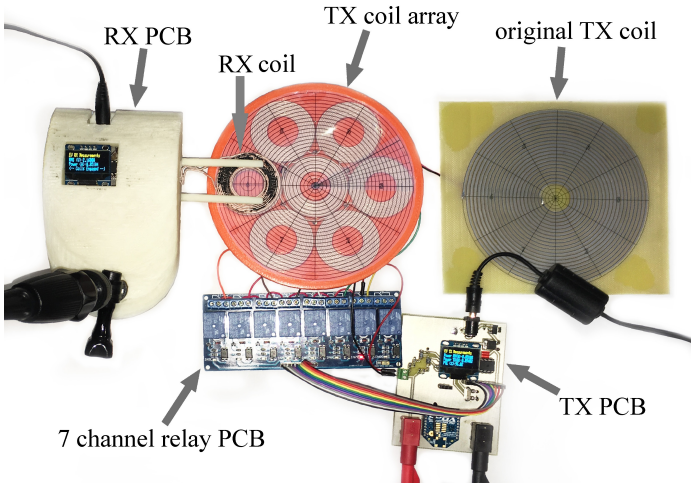

Fig. 3: Small-scale hardware prototype of EV WPT system

The proposed coil design consists of a collection of smaller coils arranged in a grid-like fashion across a flat surface as shown in Fig. 4. A_{1-7} mark the centre of each inscribed circle and represent the TX array coils. The large black circle represents a traditional TX coil. R_P is the radius of the original benchmark coil, and r_P is the radius of the proposed smaller coils. As the RX coil is placed at an arbitrary location above the array, simulating the vehicle's parking misalignment, only the nearest TX coil is energized and transmits power to the EV. To illustrate this, C_{1-4} represent stopping locations at regular intervals from the arrays centre to its outer edge. When the vehicle stops at C_3, only coil A_2 is energized, for example. This adaptive switching between smaller TX coils, effectively

halves the misalignment distance when compared to the larger single coil design.

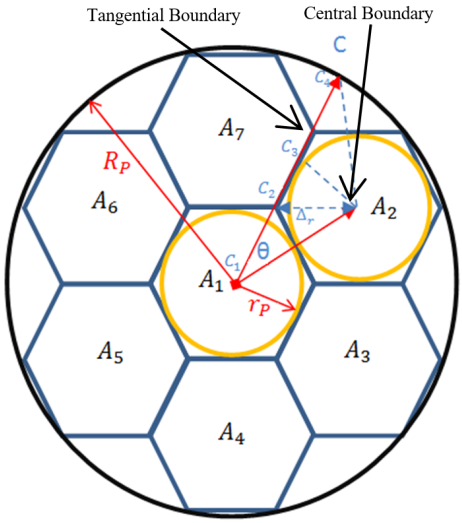

Fig. 4: The proposed TX coil array design: the RX resonant coil is mounted on the EV, the TX array is embedded beneath the road surface.

As shown in Fig. 4, the array has two possible paths for the RX coil to follow during misalignment, referred to as central and tangential boundaries. If the receiver stops along the central boundary, the two resonant coils will have the shortest misalignment distance, therefore maximising PTE. The tangential boundary represents the worst case scenario as it contains a triangular gap where the misalignment distance is at its maximum and thus PTE is reduced. Future experiments will attempt to improve this by using an overlapping coil configuration.

IV. Simulation & Experimental Results

This section evaluates the experimental results from PTE measurements taken for lateral misalignment Δ between the RX coil and TX array structure and compares these to the larger TX benchmark coil. A further comparison is made between experimental data, simulation results and theory. Angular misalignment was neglected as it is unlikely to occur due to the parallel nature of charging coils in a practical EV scenario.

Using the mathematical model for PTE discussed in Section II, and the software package MAPLE16, theoretical PTE values for each point C_x were calculated, where subscript x represents regular points along the radius of the array as shown in Fig. 4. An equivalent circuit of the misaligned MRC-WPT system was then simulated in ADS 2012. The inductance, capacitance and resistance of the resonant coils were calculated using equations (1), (2) and (3).

Fig. 5a and 5b show the relationship between PTE and the misaligned distance Δ for the theoretical calculations + simulations and experimental results respectively. The simulated model and small-scale experimental setup used a RX coil radius R_o of 0.5 m and 22 mm respectively. Therefore,

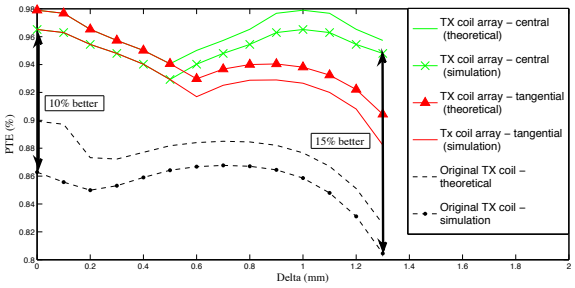

(a) Simulation and Theory

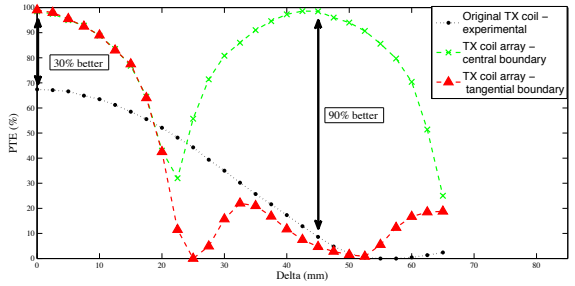

(b) Experimental Results

Fig. 5: Relationship between PTE and Δ. Simulation and theory results shown in (a) use a radius of 1.5 m for the original TX coil and 0.5 m for the proposed TX array coils. Experimental results shown in (b) use 75 mm and 22 mm respectively.

the comparison focuses on data trend and relative PTE improvements rather than absolute values.

The results obtained from simulations broadly agree with the theory and show that:

- The proposed coil array achieves a higher PTE compared to a single TX coil in each misaligned position, with an increase of 10% and 15% at the centre and outer edges respectively as shown in Fig. 5a.
- A "valley" exists in the proposed coil array between Δ = 0.4 m and 0.7 m, as this is where the RX coil's centre is furthest away from any array coil.

For the experimental setup, PTE readings were taken along a horizontal line from the array's centre to its outer radius (R_o = 65 mm) in 2.5 mm intervals and were repeated for $0-360°$ at increments of $5°$. The vertical displacement (D) between TX and RX coils was kept constant at 1 mm. The results were plotted on a 2D graph and on a heat map using MATLAB.

As shown in the heat map in Fig. 6, the tangential boundary contains a triangular gap between Δ = 22.5 to 30 mm, where the PTE was shown to dip below 15% due to a lower coupling coefficient between TX and RX coils. As previously discussed, this could easily be solved using an overlapping array.

The central boundary, however, marks a region where PTE was much higher for any given location of the RX coil along this line. The heat map shows that the PTE achieved at Δ = 45 mm was 98.5%, whereas the benchmark single coil only achieved 8.5%. Thus an increase of 90% PTE was observed

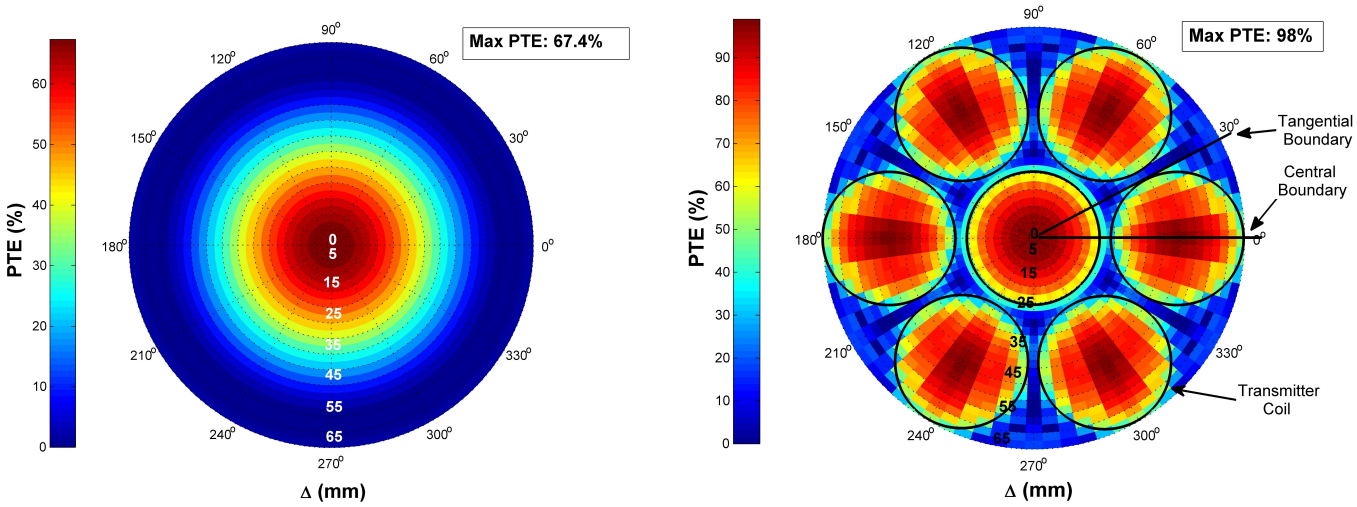

(a) Original single TX coil

(b) Proposed TX coil array

Fig. 6: Heat map showing relationship between PTE and Δ for the original TX coil (a) and the proposed TX array coils (b). The TX coil R_p is 65 mm and the array coil r_p is 22 mm.

even when the RX coil was misaligned by $3/4$ of the array radius.

Since the coil properties used in the simulations and experiments were different (e.g. dimensions, L, Q-factor), the significance of these results is even more powerful; i.e. the new array design successfully achieved a higher PTE in different scenarios whilst confirming identical trends for PTE vs. Δ.

V. Conclusion

The success of MRC-WPT in EV's relies on adequate alignment of TX and RX coils, to ensure high PTE and to minimise the losses incurred by both customers and electricity providers. There are many parameters of the coils that affect PTE such as its location, dimensions and geometry. This paper introduces a novel array-type primary resonant coil design, which solves the misalignment issue in MRC-WPT and achieves a higher PTE. In practice, coil misalignment is inevitable, since it is difficult for drivers to accurately park their car above a designated charging point or stay within dynamic charging boundaries. Experimental results were obtained using custom designed hardware and showed a clear trend between the theory and real-world implementation of the proposed array design. PTE improvements were observed, of up to 20% in simulations and between 30-90% in the experimental setup. Furthermore, the array design can reduce the RX coil radius and thus reduce the cars weight. Another advantage is the flexibility in choosing any number of TX array coils and varying their arrangement. However, this paper only considers the case where a single TX coil in the array is energized at any time. Future work will explore the powering of multiple coils and design of an overlapping array structure. Furthermore, the proposed coil design will be applied to a dynamic charging system.

Acknowledgments

The authors acknowledge Difu Shi, Minglei You, and the technician staff of Durham University for their assistance during the project.

References

[1] L. Xie, Y. Shi, Y. Hou, and A. Lou, "Wireless power transfer and applications to sensor networks," *IEEE, Wireless Communications*, vol. 20, no. 4, pp. 140–145, August 2013.

[2] Y. Zhang, Z. Zhao, and K. Chen, "Frequency decrease analysis of resonant wireless power transfer," *IEEE Transactions on Power Electronics*, vol. 29, no. 3, pp. 1058–1063, March 2014.

[3] X. Mou and H. Sun, "Wireless power transfer: Survey and roadmap," in *proc. of 81st IEEE Vehicular Technology Conference*, May 2015, pp. 1–5.

[4] S. Li and C. Mi, "Wireless power transfer for electric vehicle applications," *IEEE Journal of Emerging and Selected Topics in Power Electronics*, vol. 3, no. 1, pp. 4–17, March 2015.

[5] K. Fotopoulou and B. Flynn, "Wireless power transfer in loosely coupled links: Coil misalignment model," *IEEE Transactions on Magnetics*, vol. 47, no. 2, pp. 416–430, Feb 2011.

[6] K. Y. Kim *et al.*, "Power transfer efficiency of magnetic resonance wireless power link with misaligned relay resonator," in *proc. of 42nd European Microwave Conference*, Oct 2012, pp. 217–220.

[7] Z. Dang and J. Qahouq, "Modeling and investigation of magnetic resonance coupled wireless power transfer system with lateral misalignment," in *proc. of 29th Applied Power Electronics Conference and Exposition*, March 2014, pp. 1317–1322.

[8] R. Jegadeesan, Y.-X. Guo, and M. Je, "Overcoming coil misalignment using magnetic fields of induced currents in wireless power transmission," in *proc. of 2012 IEEE MTT-S International in Microwave Symposium Digest*, June 2012, pp. 1–3.

[9] H.-C. Son, J.-W. Kim, Y.-J. Park, and K.-H. Kim, "Efficiency analysis and optimal design of a circular loop resonant coil for wireless power transfer," in *proc. of 2010 Asia-Pacific Microwave Conference*, Dec 2010, pp. 849–852.